An Experimental Characterization of Thermophysical Properties of a Porous Ceramic Shell Used in the Investment Casting Process

C. A. Jones , **M. R. Jolly, A. E. W. Jarfors** and **M. Irwin**

Abstract This study presents the results of an investigation that characterises the thermophysical properties of an investment casting mould, comprising of a Zirconium dioxide/Cobalt aluminate prime slurry and a fused Silica/fibre reinforced backup slurry. Growing prevalence of successful computer simulations within the foundry industry enables defects that emerge during the casting process to become increasingly predictable, providing cost-effective alternatives to trial castings. The viability of these simulations as predictors is heavily dependent upon the facilitation of accurate material property data, as attained through this investigation. Differential scanning calorimetry (DSC) and laser flash analysis (LFA) were utilized to determine the specific heat capacity and thermal diffusivity, respectively. These values, in combination with the material density and linear coefficient of thermal expansion, have been used to determine the thermal conductivity of the mould. With the aim of verifying these parameters, initial studies in Flow-3D® simulation software have been performed to determine the constraints needed to reduce variability in simulation parameters. Due to the diversity of casting moulds used throughout the industry, ensuring the material database is kept as comprehensively populated as possible is a crucial undertaking.

Keywords Component casting · Thermophysical properties · Conductivity · Porosity · CFD simulation · Sustainable

C. A. Jones (✉) · M. R. Jolly
Sustainable Manufacturing System Centre, Cranfield University, Bedfordshire MK43 0AL, UK
e-mail: c.a.jones@cranfield.ac.uk

A. E. W. Jarfors
School of Engineering, Jönköping University, Box 1026, 551 11 Jönköping, Sweden

M. Irwin
TPC Components AB, Brånstaleden 2, 734 32 Hallstahammer, Sweden

Introduction

Investment casting is the preferred manufacturing technique for the production of high-quality components for aerospace applications as a result of the geometric complexity and dimensional tolerances it affords [1]. As computers become more powerful, the process of optimizing the production of such complicated parts has gradually been moving from the traditional trial and error approach [2], utilized by foundries of old, to much more resource-efficient computer simulations.

Any computer simulation is only as accurate as the physical parameters underpinning its predictive capabilities. A comprehensive understanding of mould thermophysical properties is crucial to obtaining any meaningful estimations of the cooling rate, temperature gradient, solidification time, microstructural development, etc. Many previous papers are concerned with the investigation of investment casting moulds, targeting mechanical properties, such as strength, using techniques including modulus of rupture (MOR) [3, 4] as well as mould creep and permeability [5]. Literature containing a comprehensive collection of material property data, especially thermophysical data, is still a rarity.

Previous research work conducted by Raza [6] on identical mould material considered the impact of fluctuations in critical process parameters introduced as a result of equipment and human involvement. His work included material characterisation and an assessment of how accurately mould filling can be predicted; however, the prediction of important solidification parameters, such as temperature gradient and cooling rate, was not assessed.

In this work, thermophysical properties have been experimentally determined for an industrial investment casting mould. The aim is to inform boundary conditions for computer simulations/verifications and, in future work, act as a basis for the prediction and statistical optimisation of microstructural development in cast components.

Methodology

The shelling system considered in this analysis is employed during the casting of Ni-based superalloys, the compositional breakdown of which is presented in Table 1. The shell consists of a prime coat supported by multiple backup layers which, generally speaking, have a combination of Zirconia and fused Silica reinforced with fibres.

Laser Flash Analysis (LFA)

A Netzsch LFA 427 instrument was used in connection with a TASC 414/4 measurement unit to determine the thermal diffusivity of the mould material.

Table 1 Ceramic mould composition

Coating	Composition	Details	
Prime	Chilches microzir flour 200 M IC	ZrO_2	>63.5%
		TiO_2	<0.2%
		Fe_2O_3	<0.15%
		Al_2O_3	<1.3%
		SiO_2	<33%
	Cobalt aluminate	$CoAl_2O_4$	100%
	Primecote® plus	Binder	
	DCH-10 antifoam	–	
Backup	Ranco-Sil 140F	SiO_2	$\approx$100%
	Matrixol 30	Binder	
	MXC excel X2	Fibre reinforcement	
	DI water	H_2O	100%

A cylindrical sample with a diameter of 12.8 mm and a height of 5.1 mm was coated with a thin layer of Graphite and Chromium before being placed in the path of a 1064 nm Helium laser, just ahead of a liquid Nitrogen cooled sensor array. The system was configured so that the sample would be heated at a rate of 50 K per minute to 1000 °C before any laser shots were conducted. Five shots were taken at each chosen temperature before the temperature was reduced by 200 °C between each group of shots.

Pycnometry

A Micromeritics AccuPyc 2 1340 Pycnometer, configured to use Nitrogen gas as opposed to Helium, was used to measure the density of the shell material as well as providing information on the shell porosity. A cylindrical sample was placed in the testing sleeve, and the computer system, operating a virtual 32-bit operating system, overseeing the equipment operation was programmed to undertake 15 repeat cycles to minimise the standard errors.

Differential Scanning Calorimetry (DSC)

A Netzsch 404 Pegasus DSC instrument was used to determine the heat capacity of the ceramic mould. Samples of mould were taken from three locations—prime coat, the approximate centre, and the outer most surface—for analysis with masses 40.4 mg, 41.4 mg, and 40.3 mg, respectively. These masses are approximately equal to 40 mg

to ensure they are comparable with the Sapphire baseline required to calculate the heat capacity.

These samples were placed individually into the testing crucible and sealed in the chamber before the atmosphere was flooded with Argon. The temperature cycle was selected to commence at 25 °C and rise to 1400 °C before returning to 25 °C at a rate of 10 K per minute.

Dilatometry (DIL)

A Netzsch 402 DIL instrument was utilized to determine the coefficient of thermal expansion (CTE) of an approximately cylindrical sample of mould material. Like the DSC, these samples must be compared to a reference sample to evaluate the CTE, a fact that limits the sample dimensions to either 12 mm or 25 mm in length with a diameter of approximately 6 mm.

One sample of each length has been tested to allow comparison of any differences between the two lengths. Individually, these samples were sealed into the experimental chamber and immersed in a Helium atmosphere. An identical temperature cycle was used in both cases in which the temperature increased to 1400 °C from the initial 25 °C before returning to 25 °C at a rate of 10 K per minute.

Results and Discussion

Laser Flash Analysis (LFA)

The mould sample that was coated solely with Graphite was not able to produce any usable results, even following multiple attempts. Such an outcome suggests that the Graphite-mould combination has significant transparency to the laser preventing the acquisition of data. Previous work has exploited such transparency at certain frequencies to monitor the filling of the mould cavity in real time [7].

A marked improvement in results was observed by coating the sample with a combination of Graphite and Chromium; the resulting thermal diffusivity measurements are illustrated in Fig. 1 alongside published experimental data from another relevant study [8]. The experimental data is in reasonable agreement with the published data lying between the two available sets with an average value of 4.64×10^{-7} m^{2}s^{-1}. The data point seen at 850 °C is the result of an unintended shot made by the computer system overseeing the instrument's operation. Only one shot was taken at this point as opposed to the five taken at all other points, and as a consequence, the associated error is significant. A second-degree least squares polynomial fitting function has been applied to the data to illustrate the data profile as a function of temperature, which takes the form as seen in Eq. 1.
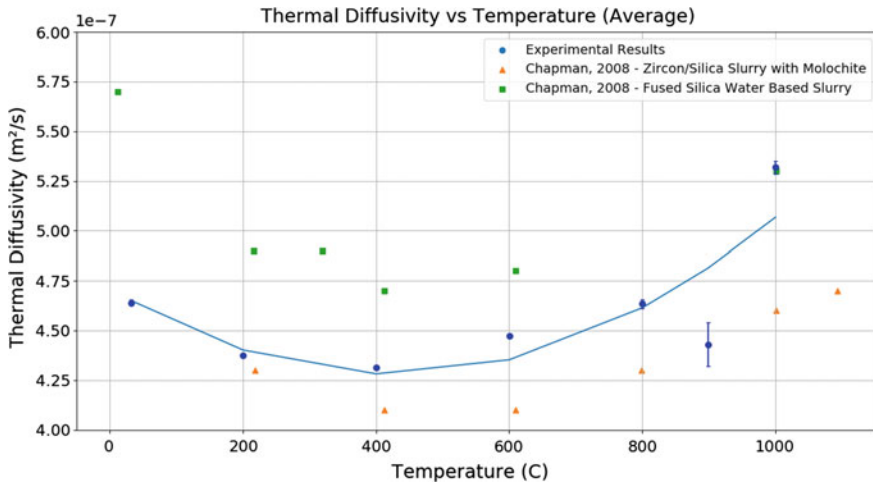
Fig. 1 Comparative plot between the experimental thermal diffusivity profile and results published in literature as a function of temperature

$$\alpha(T) = 2.39 \times 10^{-13} T^2 - 2.03 \times 10^{-10} T + 4.71 \times 10^{-7} \tag{1}$$

It was intended to attain thermal diffusivity results for temperatures up to and including 1500 °C; however, even with the Chromium coating, it was not possible to gather data above 1000 °C. It might be possible to solve this issue by using powdered shell samples in place of the intact samples, a technique that can be employed when using LFA equipment.

Differential Scanning Calorimetry (DSC)

DSC results were obtained independently for each of the three samples taken from the shell specimen, representing different regions within a typical shell. To estimate the overall heat capacity of the shell, a rule of mixtures approach (Eq. 2) was used which has been presented in the published literature as an appropriate technique when considering ceramic materials [9].

$$C_p^{\text{eff}} = \sum_i \left(\frac{A_i M_i}{A_1 M_1 + A_2 M_2 + A_3 M_3} \right) C_p^i \tag{2}$$

Here, C_p^{eff} is the effective specific heat capacity, i is an integer ranging in value from 1 to 3 denoting the innermost sample, centre sample, and the outer most sample, respectively, A_i is a mass-dependent scaling coefficient, M_i is the sample mass, and C_p^i is the specific heat capacity.
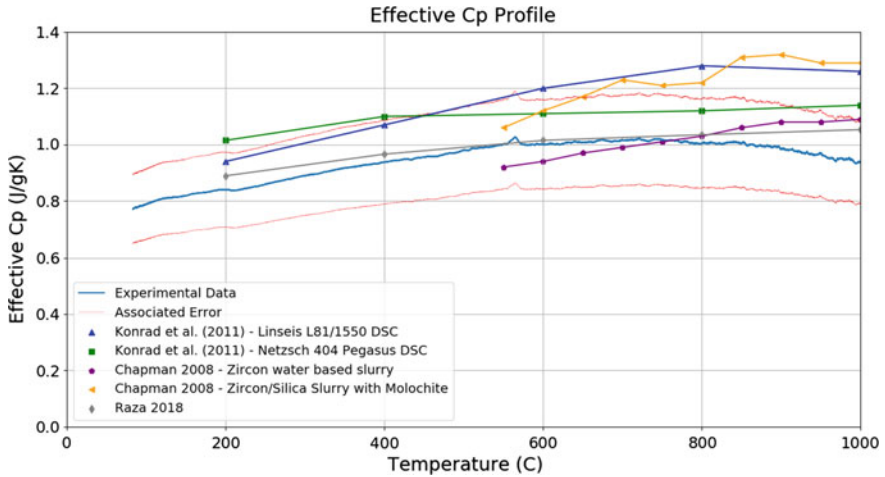
Fig. 2 Comparative plot between the experimental C_p data and previous results from the literature as a function of temperature

An important consideration in the scaling coefficient, A, is whether it should be considered as a mass or volume-dependent term. Physics tells us that the specific heat capacity defines the energy required to raise the temperature of 1 kg of material by 1°K, illustrating the clear reason for allocating a mass dependency over volume dependency.

Figure 2 shows the results of the specific heat capacity measurements including the calculated scaling factors of the three layers; $A_1 = 0.0548$, $A_2 = 0.9273$, and $A_3 = 0.0179$, respectively. These factors were evaluated by determining the mass of like layers relative to the total mass of the sample. Given the output volume of data points, a region of uncertainty, bounded by the lines in red, was selected as opposed to presenting an individual error at each point.

Plotted alongside the experimental results are data published from Chapman et al. [8] and Konrad et al. [10]. The comparison between the results and published data, particularly with the trend of the [10] (Netzsch instrument) and Raza [6], is in very good agreement. In the temperature region approaching 1000 °C, the results of C_p^{eff} begin to drop relative to the other data sets, with the exception of Konrad et al. [10] (Linseis instrument) data which plateaus and begins to fall in a similar manner. Such a trend was not expected and may well be caused as a result of the technique for modelling heat capacity.

Our experimental results generally form an uninterrupted curve comparable to those seen in the literature; however, a pronounced peak emerged in the profile at ≈150 °C. Although the weighting factors have eliminated this peak, they have revealed a second, much smaller peak which is visible in Fig. 2 at ≈550 °C. Peaks appearing in a DSC profile can be directly attributed to chemical reactions/phase changes that occur between mould components. This remaining peak at ≈550 °C is most likely the result of transitions between polymorphs of Silica, specifically

between α-quartz and β-quartz at 573 °C [11]. The suppressed peak at the lower temperature is also more than likely attributable to Silica as transitions are possible at a temperature as low as 117 °C [11]. Due to the slow speed of the temperature changes during the experiment, this phase transformation is fully reversible; hence, why the lower temperature peak appeared in both the increasing and decreasing cycles of temperature.

Dilatometry

As both a 12 mm and 25 mm sample were investigated during a heating and cooling phase, four profiles of fractional length change against temperature are available to consider. As indicated by Eq. 3,

$$\frac{\mathrm{d}L}{L_0} = \alpha \Delta T \tag{3}$$

where dL is the sample change in length, L_0 is the original sample length, α is the linear coefficient of thermal expansion, ΔT is the change in temperature, and the CTE can be determined by taking the gradient of these profiles. This was performed for all four profile where the local CTE was determined at 100 °C intervals to create a plot of CTE against temperature, and a statistical assessment was conducted to assess the extent to which these data sets represent a statistically viable result. SPSS software was used to perform a linear regression and an analysis of variance (ANOVA) test on each data set, and the R^2 and p values were recorded. We would expect CTE to be independent of temperature and hence there to be no significant correlation between these factors. Correlations were deemed significant when p<0.05. These tests reveal that of the four available data sets only the 12 mm and 25 mm samples during the increasing temperature cycle showed a non-correlating relationship giving values of 2.31x10^{-6} K^{-1} and 3.50x10^{-6} K^{-1} respectively (25mm: F(1,10)=0.531, p=0.483, R^2=0.05; 12mm: F(1,10)=2.82, p=0.132, R^2=0.26). It should be noted that the inhomogeneity of the material causes high variation in the CTE that should be investigated further in future work.

Taking gradients of these results has a high sensitivity to noise in the experimental setup if conducted across narrow ranges in temperature. This is due to the fact that large fluctuations are present within very narrow ranges. Performing the assessment across a wider temperature range (± 5°C) generates results that are both visually and statistically more in keeping with the expected linear fitting expected from Eq. 3.

The uncertainty in the CTE measurement using directly comparable equipment has been discussed in the previously published literature [12]. From this work, the uncertainty was determined using the Guide to the Expression of Uncertainty in Measurement to have a value of 5.8×10^{-8} K^{-1} independent of the measured value.

Density and Porosity

The resulting density determined from the Pycnometry experiment has a value of 2.536 ± 0.002 gcm^{-3} and a porosity value a 60.568%. Although not identical in composition, density measurements quoted in literature [13] for similar shell materials have a lower value: 1.93 gcm^{-3} for Alumina-Silica mix and 1.64 gcm^{-3} for Zircon-Silica mix. The difference in density can be explained by the use of Zirconia in this study over Zircon in [13]. Zirconia has a higher density relative to Zircon, resulting in a higher overall shell density.

The porosity value is significantly higher than a 31.7% porosity value quoted by Xu [13]. Unlike this source however, the porosity of the shell under consideration in this work increases during firing as the fibre reinforcements burn away. As a result, it is not necessarily surprising that the porosity value is so much higher than those of other studies.

Thermal Conductivity

Based on measurements of density, heat capacity, and thermal diffusivity, it was possible to calculate the thermal conductivity, shown graphically in Fig. 3, of the material using Eq. 4 [14].

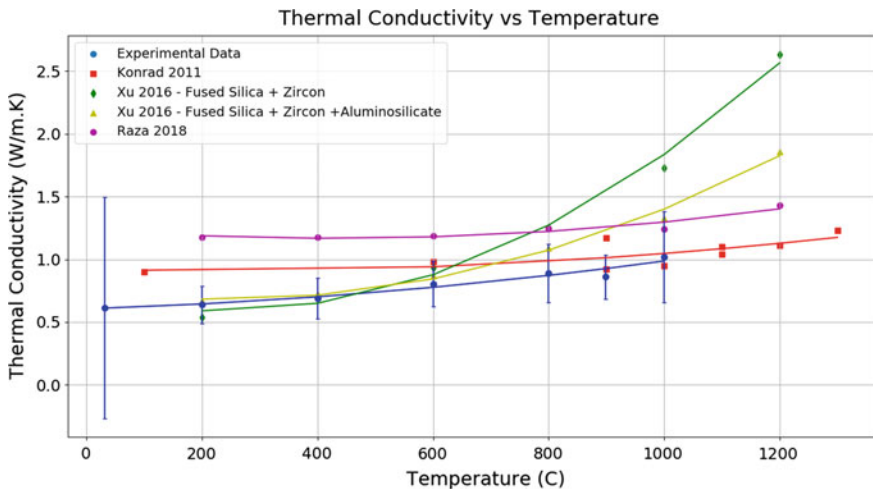$$\lambda = \rho C_P \alpha \tag{4}$$

Fig. 3 Comparative plot between the calculated thermal conductivity and thermal conductivity data published in literature sources as a function of temperature

Here, λ is the thermal conductivity, ρ is the density, C_P is the heat capacity, and α is the thermal diffusivity. As a direct consequence of the limited results from the LFA, thermal conductivity is limited to the same 1000 °C temperature value. Included in Fig. 3 is data for similar shell materials gathered from previously published literature [10, 14]. Despite an exceptional agreement between our experimental C_p results and other data from [6], the calculated thermal conductivity results fall below those seen in [6] except for the high temperature measurement, which is not necessarily reliable (as a result of LFA complications). Generally, the calculated data is in good agreement with the collection of results from the literature with an average value of 0.789 $Wm^{-1}K^{-1}$ and conforms to the same trend of increasing with temperature.

Computational Verifications

Commercial computer software, specifically Flow-3D®, was employed to verify the experiment results. Unfortunately, as it has not yet been possible to organise a full-scale casting experiment there is no possibility of making comparisons between experimental and simulation results. However, as the primary purpose of this characterization work is to inform simulation boundary conditions, aspects of the configuration for such simulations that have been completed are worthy of discussion.

Mesh Analysis

The sensitivity of simulations to the mesh that is established around the geometry is an important consideration initially due to the dramatic effects it can have on computational times and accuracy; this is particularly true when dealing with thin casting cross sections. Previous literature surrounding mesh analysis [15] indicates that an examination of both the mesh element dimensions and the time-step is necessary to consider a simulation sufficiently optimized.

After conducting trials, it was concluded that a dual mesh configuration was the most appropriate where a coarse mesh was placed over the downsprue and ingates and a fine mesh placed over the thin section of the component. The final dimensions of the coarse and fine meshes were 1 mm × 1 mm × 1 mm and 0.5 mm × 0.5 mm × 1 mm, respectively, with a time-step of 1×10^{-5} s.

Conclusion

With the appropriate use of scientific instrumentation, it has been possible to determine a comprehensive set of thermophysical properties for an industrial investment casting shell.

These techniques are however not necessarily infallible during implementation with factors including the interaction between shell and equipment having a profound effect on the results. Although not all issues have been overcome, values of the linear coefficient of thermal expansion, density, porosity, thermal diffusivity, and thermal conductivity were determined as a function of temperature. These values are fundamental foundations for building accurate computer simulations to assess and ideally reduce defects in cast components.

Future work will include comparisons between experimentally obtained data and Flow-3D® computer simulations to verify the findings. In addition, further investigations are intended on the LFA to determine values of the thermal conductivity as a function of temperature in the range above 1000 °C.

References

1. Jolly M (2003) Castings. In: Karihaloo B (ed) Comprehensive structural integrity. Elsevier, Oxford, pp 377–466
2. Kuljanic E (2005) (ed) Advanced manufacturing systems and technology. Springer, Wien, New York
3. Hendricks MJ, Wang PMJ, Filbrun RA, Well DK (1998) Hot MOR and creep properties of common ceramic shell refractories. In: 46th annual technical meeting of the investment casting institute
4. Wolfe CM, Holubik KL, Hendricks MJ, Wang PMJ (2010) How ceramic shell properties predict resistance to shell cracking, pp 1–16
5. Hendricks MJ (1990) An analysis of ceramic shell materials. In: 21st European conference on investment casting
6. Raza M (2018) Developing process design methodology for investment cast thin-walled structures. Malardalen University
7. Gebelin J, Jolly MR (2001) Modelling filters in investment casting. In: FOCAST 2nd mini conference
8. Chapman LA et al (2008) Properties of alloys and moulds relevant to investment casting
9. Jones S (2000) Summary of standard shell properties obtained for inclusion in modelling development. In: FOCAST 1st mini conference
10. Konrad CH, Brunner M, Kyrgyzbaev K, Völkl R, Glatzel U (2011) Determination of heat transfer coefficient and ceramic mold material parameters for alloy IN738LC investment castings. J Mater Process Technol 211(2):181–186
11. Gornostayev S, Kerkkonen O, Harkki JJ (2006) Importance of mineralogical data for influencing properties of coke. Process Metall 770–773

12. Matsushita T, Ghassemali E, Saro A, Elmquist L, Jarfors A (2015) On thermal expansion and density of CGI and SGI cast irons. Metals (Basel) 5(2):1000–1019
13. Xu M (2015) Characterization of investment shell thermal properties
14. Xu M, Lekakh SN, Von Richards L (2016) Thermal property database for investment casting shells. Int J Met 10(3):342–347
15. Pohanka M, Woodbury KA, Woolley J (2002) Obtaining temperature-dependent thermal properties of investment casting mold. In ASME international mechanical engineering congress and exposition